Features of the optical absorption, phonon spectrum and glass transition in As-Se, As-Se-S, As-Se-Te chalcogenide semiconductors

R. I. ALEKBEROV[a,b,*], A. I. ISAYEV[a], S. I. MEKHTIYEVA[a]
[a]*Institute of Physics named after academician G. M. Abdullayev's of Azerbaijan National Academy of Sciences, G. Javidave 13, AZ1143 Baku, Azerbaijan*
[b]*Azerbaijan State University of Economics (UNEC), st.Istiqlaliyyat 6, Baku, AZ 1001, Azerbaijan*

The optical properties, phonon spectrum, amorphousness and glass transition temperature of $As_{40}Se_{60}$, $As_{40}Se_{30}Te_{30}$, $As_{40}Se_{30}S_{30}$, $As_{33,3}Se_{33,3}S_{33,4}$, $As_{33,3}Se_{33,3}Te_{33,4}$ chalcogenide glasses have been studied by optical, Raman spectroscopy, X-ray diffraction and differential scanning calorimetry (DSC) methods. Ithas been determined the values of optical band gap(Eg), energy of Urbach(U), the bands of Raman scattering, glass transition temperature(Tg) and also was calculated the parameters characterizing the amorphous matrix as cohesive energy(CE), the average bond energy($\langle E \rangle$) average coordination number(Z), the average value of the atomic volume (Va), packing density (ϰ) and compactness (δ) in studied compositions. The results show that, there is correlation between the cohesive energy (CE), the glass transition temperature(Tg), the average bond energy ($\langle E \rangle$) and the optical band gap (Eg).

(Received January 14, 2020; accepted December 7, 2020)

Keywords: Chalcogenide, Glass, Amorphous, Cohesive energy

1. Introduction

The intensively increase in the number of work devoted to the study of the structure and physical properties of chalcogenide glassy(ChG) semiconductors due to their promising for use in a variety of infrared optical devices, such as infrared optical fibers, planar waveguides, fiber amplifiers, optical and electrical switches, lasers, etc [1-3, 4, 5].This contributes to their unique physical properties, in particular, the transparency in the visible and near infrared regions of the spectrum, high photosensitivity, nonlinear refractive index, as well as low values of phonon energy, the simplicity of the technological process and the chemical resistance.The majority of studies concerning the chalcogenide glasses performed mainly in As_2Se_3, As_2S_3 and other binary compounds [1-9]. The structural, electrical and optical properties have been studied in detail for these materials. The addition of the third and fourth components to binary chalcogenide glass compounds allows us to expand the range of variation of physical properties, as well as the area of their application. In particular, the ternaryAs-Se-S chalcogenide glassy systems are distinguished by an extended transparency region and high non-linear properties [10].The As-Se-Te chalcogenide glasses havehigh refractive index and good transparency in the middle and far area of the infrared spectrum [11]. However, the success of the implementation of applied depends on understanding the mechanism of physical processes occurring in it, on the ability to control the physical properties, which can be achieved by establishing a correlation between properties and structure. Besides, it is essential to determine the methods of obtaining materials that have stable physical properties. The optical band gap and glass transition temperature is considered to be an important parameter characterizing the glassy state and is directly connected with rigidity of amorphous matrix. Therefore, special attention was paid to the establishment of a correlation between these quantities and other physical parameters characterizing the rigidity of an amorphous matrix, in particular, the coordination number, the average bond energy, cohesive energy, the compactness structure, the average molar volume, etc. The great number studies of this kind have been carried out by many authors [12–17] and proposed formula relating the glass transition temperatures with the coordination number and average bond energy.The selected compositions for studies differ little in the mean value of the coordination number (respectively are 2.4 and 2.33 for stoichiometric and non-stoichiometric compositions), but contain chemical bonds differing in bond energy, which will establish correlations between optical and other physical parameters.

In this article are synthesized the As_2Se_3, $As_{40}Se_{30}S_{30}$, $As_{40}Se_{30}Te_{30}$, $As_{33.3}Se_{33.3}S_{33.4}$, $As_{33.3}Se_{33.3}Te_{33.4}$glass compositions and thin films (d=1÷3mkm) are obtainedby thermal evaporation in vacuum from the synthesized materials.The experiments have been carried out to measure the transmission spectra, the glass transition temperature and density, Raman scattering.

2. Experimental details

2.1. Sample preparation

The glassy samples with compositions of $As_{40}Se_{60}$, $As_{40}Se_{30}Te_{30}$, $As_{40}Se_{30}S_{30}$, $As_{33.3}Se_{33.3}Te_{33.4}$,$As_{33.3}Se_{33.3}S_{33.4}$ were synthesized from 5N purity elements by the conventional melt-quenching method. The components of a proper composition were placed in a quartz ampoule, which was evacuated to a residual pressure of 10^{-3} Pa. The synthesis were performed in a rotary furnace as the ampoules were heated up to 950 °C and kept at this temperature for 12 h, the furnace was rotated for homogeneous melting. After finishing the synthesis, the ampoules were pulled out and were quenched in air, part of the samples was powdered for the X-ray diffraction studies. The amorphous of the films was checked by X-ray diffraction analysis. The broad maxima observed in the diffraction curves are indicated by the absence of crystallized areas (Fig. 1).

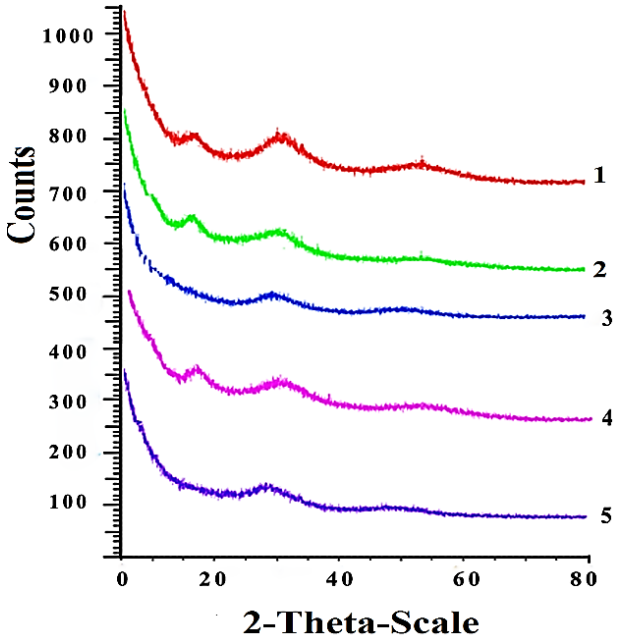

Fig.1. X-ray curves of powder glass compositions: 1-$As_{40}Se_{60}$, 2-$As_{40}Se_{30}S_{30}$, 3-$As_{40}Se_{30}Te_{30}$, 4-$As_{33,3}Se_{33,3}S_{33,4}$, 5-$As_{33,3}Se_{33,3}Te_{33,4}$ (color online)

Densities of chalcogenide glasses, ρ were calculated using the formula:

$$\rho = \left[\frac{w_0}{w_0 - w_L}\right]\rho_L \qquad (1)$$

where,w_0 and $w_L$the weight of the sample in air and in liquid (water) and density of liquid (water) is equal to 1 g/cm3 at room temperature. The density of $As_{40}Se_{60}$, $As_{40}Se_{30}Te_{30}$, $As_{40}Se_{30}S_{30}$, $As_{33.3}Se_{33.3}Te_{33.4}$, $As_{33.3}Se_{33.3}S_{33.4}$glass materials was measured by Archimedes' principle using liquid (water). The accuracy was better than± 0.02 g/cm3.

2.2. Optical experiments

The transmission spectra of the thin films in the spectral range 190-1100 nm were obtained using ultraviolet visible-near infrared spectrophotometer (SPEKOL-1500). The spectrophotometer was set with a slit width of 2 nm. All the measurements reported were taken at room temperature. The chalcogenide glasses have been thermally evaporated with an evaporation rate of ~0.6 nm/s in vacuum at residual pressure of $1.33x10^{-4}$ Pa. The substrates used in this study were optical glasses (BK7) ultrasonically cleaned before deposition process. The thickness of the films was 2 μm, determined by the Carl ZeissSigma VP Scanning Electron Microscopy (SEM) measurements.

2.3. Raman scattering experiments

Amorphous films of all compositions and thicknesses ~10 μm were prepared by thermal evaporation with the deposition rate 0.4–0.5 μm/min on glass substrates in vacuum under the pressure 10^{-4}Torr. Raman studies were carried out on three-dimensional Confocal Laser Microspectrograph (Tubitak, Turkey). The excitation source was He-Ne laser (25 mW) operating at a wavelength of 632.8 nm. Cross-section radius of laser beam incident on the film sample was ~1 μm. Exposure time was 1–90 s.

2.4. Differential scanning calorimetric experiments

The glass transition behavior of $As_{40}Se_{60}$, $As_{40}Se_{30}Te_{30}$, $As_{40}Se_{30}S_{30}$, $As_{33.3}Se_{33.3}Te_{33.4}$, $As_{33.3}Se_{33.3}S_{33.4}$ chalcogenide glassy have been studied by carrying out differential scanning calorimetry (DSC). Measurements were performed on the STA-6000 Simultaneous Thermal Analyzer and the samples heated at a rate of 30 °C/min. The sample was heated at a rate of 30 °C/min. A typical sample weight was about 15 mg. An empty aluminum pan was used as a reference sample and matched the sample pans by ±0.15 mg. The heating schedules consisted of a heating scan from T_0= 25 to 300 °C at heating rate 30 °C/min

3. Results

3.1. Optical results

Fig.2a shows the optical absorption spectra of $As_{40}Se_{60}$, $As_{40}Se_{30}Te_{30}$, $As_{40}Se_{30}S_{30}$, $As_{33.3}Se_{33.3}Te_{33.4}$, $As_{33.3}Se_{33.3}S_{33.4}$glass compositions.The optical absorption spectrum of ChG materials consists of three areas the dependence of the absorption coefficient (α) on the photon energy [18-19]. The weak absorption area (α <1 and is weakly dependent on the energy of the photon) for low values of the energy of the photon, the intermediate region obey the law Urbach (α ~ $1 \div 10^3$ cm^{-1}) [20] and area of high values of the photon energy (hν>Eg , Eg – is the optical band gap) is corresponding to Tauc's low (Fig. 2b);

$$\alpha \cdot h\nu = B(h\nu - E_g)^n \qquad (2)$$

where, Eg and B correspond to the optical band gap and the slope of the graph, ν –is the frequency of the incident light, h -is Planck's constant. The values of index (n) depend on the nature of the electronic transitions, whichforstudiedcompositionsis equal 2 and indicate the nature of indirect optical transitions [19].

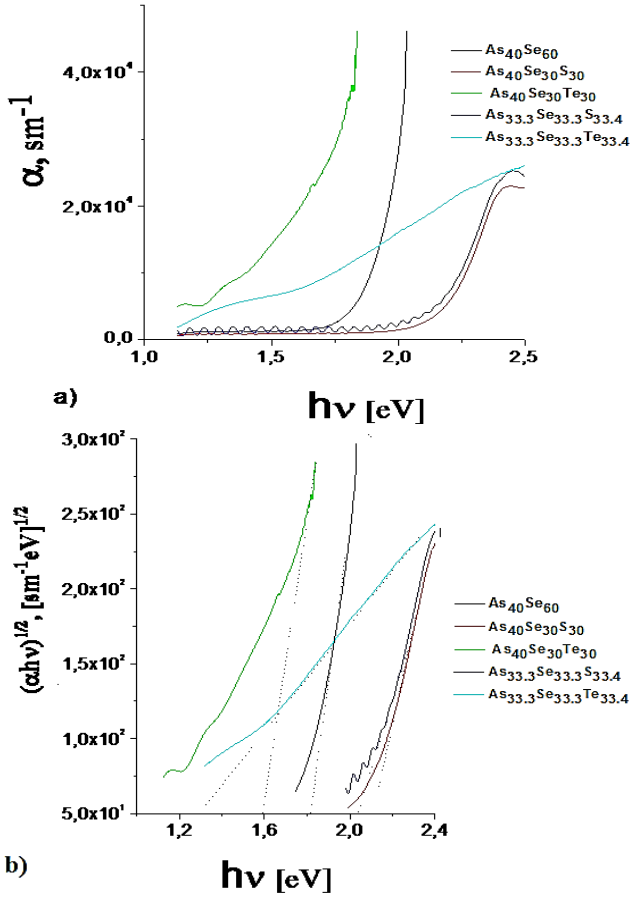

Fig.2.The optical absorption spectra of $As_{40}Se_{60}$, $As_{40}Se_{30}Te_{30}$, $As_{40}Se_{30}S_{30}$, $As_{33.3}Se_{33.3}Te_{33.4}$, $As_{33.3}Se_{33.3}S_{33.4}$ chalcogenide glasses(a) and variation of $(\alpha h\nu)^{1/2}$ versus photon energy (hν)(b) (color online)

It was plotted the graphs of the absorption spectra from the region obeying Tauc's law as a dependence $(\alpha \cdot h\nu)^{1/2} \sim f(h\nu)$ and have been determined the values of Eg by extrapolation to the axis of abscissa and the value of parameter B from the slope of the graph (Fig.2b). Besides, have been presented as a dependence $\ln\alpha \sim f(h\nu)$ (Fig. 3), corresponding to the Urbach area and captured at different temperatures, where the absorption coefficient exponentially depends on the energy of the incident photon and is expressed by the formula:

$$\alpha = \alpha_0 \exp\left[\frac{\sigma(h\nu - E_0)}{kT}\right] = \alpha_0 \exp\frac{h\nu - E_0}{U} \qquad (3)$$

By using a formula (3) was determined the Urbach energy (U= σ/kT) (inverse of the slope of the absorption edge $U^{-1} = (\Delta(\ln\alpha)) / (\Delta(h\nu))$), the steepness parameter of the absorption edge(σ), as well as the coordinates (α_0 and E_0) of the point of convergence of the Urbach bundle (convergence point of the Urbach bundle). Their values are presented in Table .1 and Table 2.

Table 1.Urbach energy (U, meV), slope of the absorption edge corresponding to the Tauc rule ($B^{1/2}$, $cm^{-1/2}eV^{-1/2}$), coordinates of the point of convergence of the Urbach bundle (α_0, cm^{-1} and E_0, eV), σ_0 Parameter of characterizing the intensity of electron-phonon interactions (σ_0)

Glass compositions	**U**	**$B^{1/2}$**	**α_0**	**E_0**	**σ_0**
$As_{40}Se_{60}$	101	1266	$4.4* 10^4$	1.99	0.28
$As_{40}Se_{30}Te_{30}$	196	904	$1.36* 10^4$	1.44	0.141
$As_{40}Se_{30}S_{30}$	152	663	$2.18* 10^4$	2.39	0.195
$As_{33.3}Se_{33.3}S_{33.4}$	153	540.6	$2.6* 10^4$	2.38	0.194
$As_{33.3}Se_{33.3}Te_{33.4}$	609	181	$1,18*10^4$	1.92	0.0457

Table 2. The effective phonon energy ($\hbar\omega_p$,meV), experimental optical band gap ($E_{g(ex)}$, eV), calculated band gap($E_{g(cal)}$, eV), band gaps of elements (E_g, eV) of studied glasses

Glass compositions	**$\hbar\omega_p$**	**$E_{g(ex)}$**	**$E_{g(cal)}$**	**E_g**
$As_{40}Se_{60}$	27,6	1.82	1.79	1.2(As)
$As_{40}Se_{30}Te_{30}$	24,5	1.59	1.274	1.99(Se)
$As_{40}Se_{30}S_{30}$	34.45	2.1	1.955	0.9(Te)
$As_{33.3}Se_{33.3}S_{33.4}$	35.32	2.04	1.8612	2.6(S)
$As_{33.3}Se_{33.3}Te_{33.4}$	24.4776	1.3	1.25907	

These parameters provide the information about the electronic, atomic configurations of ChG materials. In the same table are described the values of the band gap calculated by the formula proposed by the authors of [21] for multi-component glasses (AxByCz):

$$E_g^r = xE_g(A) + yE_g(B) + zE_g(C) \qquad (4)$$

where x, y and z are volume fractions, and -$E_g(A)$,$E_g(B)$, $E_g(C)$ are the band gaps of elements A, B, and C.

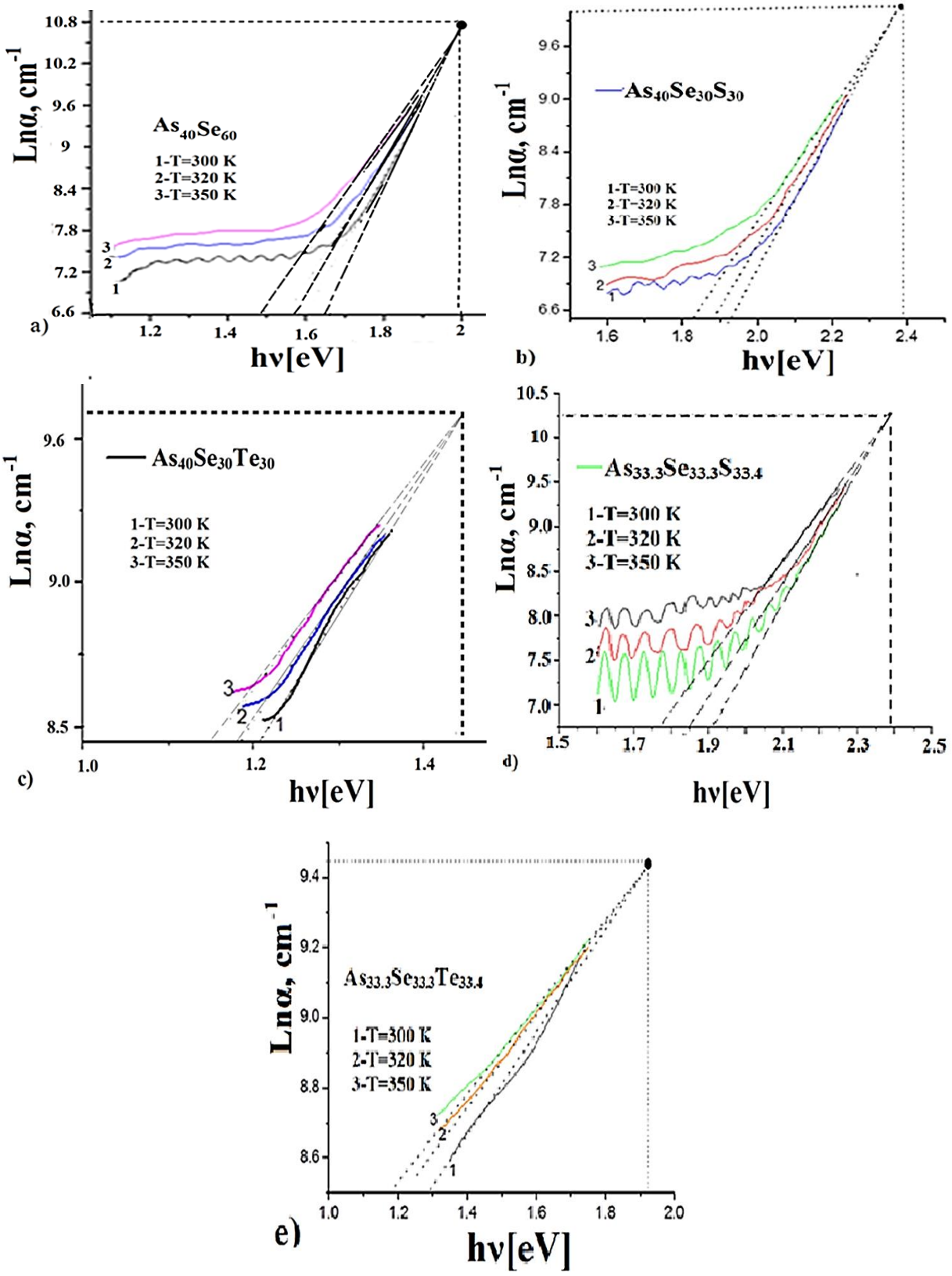

Fig.3.Theoptical absorption spectra dependenciesofAs_2Se_3(a), $As_{40}Se_{30}S_{30}$(b), $As_{40}Se_{30}Te_{30}$(c), $As_{33,3}Se_{33,3}S_{33,4}$(d), $As_{33,3}Se_{33,3}Te_{33,4}$(e) glasses for the different temperatures at the Urbach absorption area (color online)

The conversion of the volume fraction in the atomic percentage is made using an atomic mass and density. The numerical values of Eg for each components included in the studied ChG compositions are presented in Table 2.

3.2. Raman scattering results

Fig. 4 shows the Raman scattering spectra for the studied ChG compositions. It can be seen from the figure that the Raman spectra undergo a significant change with change of the chemical composition.

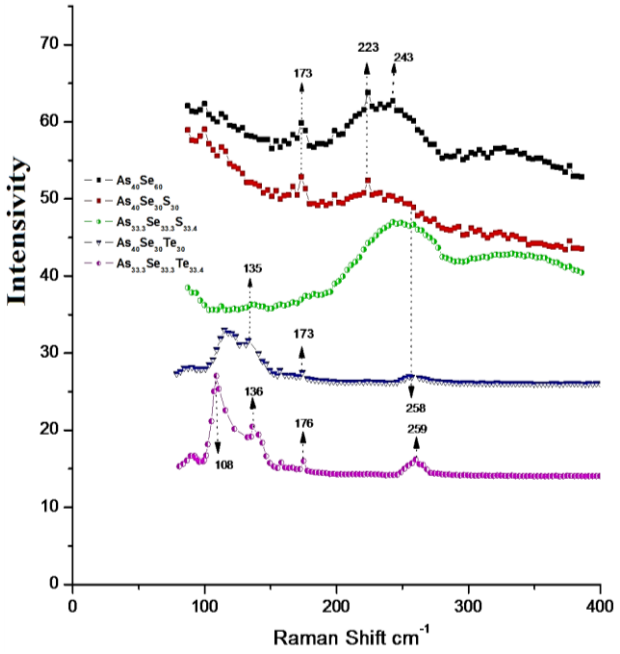

Fig.4. Raman spectrum of $As_{40}Se_{60}$, $As_{40}Se_{30}S_{30}$, $As_{40}Se_{30}Te_{30}$, $As_{33,3}Se_{33,3}S_{33,4}$, $As_{33,3}Se_{33,3}Te_{33,4}$glass compositions (color online)

The spectrum of $As_{40}Se_{60}$ glass composition contains the band covering the frequency range of 195 ÷ 295 cm^{-1} and the peak at 223 cm^{-1} belonging to the main AsSe3 structural element forming the amorphous matrix [22, 23]. Slightly pronounced peaks in the range of 238 ÷ 258 cm^{-1} are associated by chain and ring selenium molecules unrelated to arsenic atoms [23,24] and band of 260 ÷ 280 cm^{-1} small peaks related to vibrations in the bridge connection between pyramidal structural units such as AsSe3, or between As4Se4 [22,25].

Thus, the amorphous matrix of $As_{40}Se_{60}$ mainly consists of heteropolar bonds between atoms As-Se and a small amount of homopolar bonds between selenium and arsenic atoms. The spectra of composition $As_{40}Se_{30}S_{30}$ contains all the bands present in the spectrum of $As_{40}Se_{60}$ with some changes, but a band appears between the maximum of 223 and 243 cm^{-1} and band covering the frequency range of 280 ÷ 400 cm^{-1}. The first band corresponds to the the main pyramidal structural elements of a pyramid, which with the difference that part of the selenium atoms are substituted by sulfur atoms. The frequency band 325–355 cm^{-1} corresponds to the pyramidal AsS_3 structural units, where some of the sulfur atoms are replaced by selenium [27, 28]. The band in the range of 380–400 $cm^{-1}$is attributed by the interaction of the AsS3 pyramids[27]. The Raman spectra of $As_{33.3}Se_{33.3}S_{33.4}$ composition contain all the bands available in the spectra of previous compositions with a different increase in the intensity of the last band and the disappearance of small sharp peaks. In all spectra, a peak is observed at frequncy 173 cm^{-1}, which is attenuated in the last spectrum. This feature is observed in all Raman scatering spectra of chalcogenide glass rich with arsenic, which is associated by structural elements containing As – As bonds [29]. The spectra of $As_{40}Se_{30}Te_{30}$ composition contains a band covering the frequency range 100 ÷ 160 cm^{-1} and maxima 110, 136, 159, 176 and 258 cm^{-1}. The maxima of 110 and 136 cm^{-1} were attributed by the asymmetric valence modes of the Se-As-Te chain, which is included in the amorphous matrix [23]. The peak at 159 cm^{-1} was also observed by the authors of [30, 31] and belongs to the vibrational modes of Te-Te the bond. The weak peak at 176 cm^{-1} corresponds to the vibrational modes of the As_2Te_3 structural units [32]. The band at 259 cm^{-1} is attributed to the vibrations of Se – Se bond [23–25, 33–34]. The Raman spectrum of $As_{33.3}Se_{33.3}Te_{33.4}$ composition contains all the features found in the spectrum of $As_{40}Se_{30}Te_{30}$ differing from that peaks at 108 and 136 cm^{-1} and a band at 259 cm^{-1} are amplified. The analysis of results show that, this fact is due to the excess concentration of chalcogen atoms.

3.3. Differential scanning calorimetry results, density of matters, thermodynamic parameters

Fig. 5 shows the differential scanning calorimetry curves of the studied ChG materials at heating rates of 20 K /min.

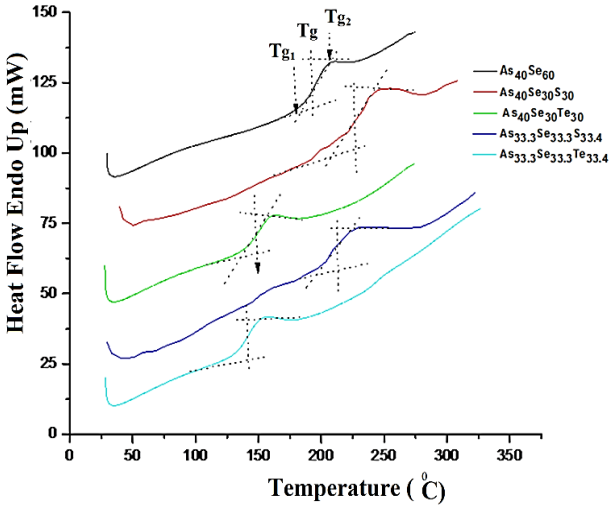

Fig.5.The DSC traces of the $As_{40}Se_{60}$, $As_{40}Se_{30}S_{30}$, $As_{40}Se_{30}Te_{30}$, $As_{33,3}Se_{33,3}S_{33,4}$ $As_{33,3}Se_{33,3}Te_{33,4}$ compositions at β = 30 K/min heating rate (color online)

The glass transition temperatures are determined by using from Fig. 5 and the results are presented in Table 3.

Table 3. Experimentally glass transition temperature ($T_{g(Ex)}$, K), empirically glass transition temperature ($T_{g(Em)}$, K) density (ρ, g/cm^3)

Glass compositions	**$T_{g(Ex)}$**	**$Tg_{(Em)}$**	**ρ**
$As_{40}Se_{60}$	465.5	388.75	4.59
$As_{40}Se_{30}Te_{30}$	421	319.9568	5.132
$As_{40}Se_{30}S_{30}$	498	421.094	3.86
$As_{33.3}Se_{33.3}S_{33.4}$	485	410.52	3.254
$As_{33.3}Se_{33.3}Te_{33.4}$	411	306.646	5.07

As can be seen from this table, undergoes a significant change the glass transition temperature with replacing some of the selenium atoms with sulfur or tellurium in $As_{40}Se_{60}$ glass composition. In the first case increases the glass transition temperature, but in the second decreases. The density were measured of all compositions, as well as the physical parameters were estimated associated with the glass transition process using the periodic tables, the coordination numbers and the known values of the density of the elements included in the studied samples, the experimental values of density for the studied compositions. The average value of the coordination number (Z), packing density (κ), the mean value of the atomic volume (Va) calculated by the formulas (5-7) and results are presented in Table 4.

Table 4. Compactness (δ, q/sm^3), average coordination number (Z), Packing density ($\chi \times 10^{22}$ atoms/cm3), average atomic volume (V_a, cm^3/mol) of the studied glasses

Glass compositions	**δ**	**Z**	**$\chi \times 10^{22}$**	**V_a**
$As_{40}Se_{60}$	−0.0075	2.4	3.57	16.85
$As_{40}Se_{30}Te_{30}$	-0.0102	2.4	3.36	17.914
$As_{40}Se_{30}S_{30}$	−0.0118	2.4	3.67	16.392
$As_{33.3}Se_{33.3}S_{33.4}$	−0.143	2.33	3.16	19.038
$As_{33.3}Se_{33.3}Te_{33.4}$	-0.02	2.33	3,249	17.9989

$$Z = \sum_i Z_i X_i A_i \tag{5}$$

$$\varkappa = \frac{\rho N_A}{\sum_i X_i A_i} \tag{6}$$

$$V_a = \frac{1}{\rho} \sum_i x_i A_i \tag{7}$$

The relative share of free volumes is often characterized by a parameter, the so-called compactness (δ) is determined by the following formula [35, 36]:

$$\delta = \frac{\sum_i (x_i A_i)/\rho_i - \sum_i (x_i A_i)/\rho}{\sum_i (x_i A_i)/\rho} \tag{8}$$

where, Z_i, x_i, A_i and ρ_i are the coordination number, molar fraction, atomic mass and density of elements included in the ChG compositions, ρ is the experimentally determined density value of the studied substances. The results are shown in Table 4. The energy of heteropolar bonds included in studied compositions and their degree of covalence are determined by formulas (9) and (10) [37-38]. The results are presented in Table 5.

$$E_{A-B} = (E_{A-A} E_{B-B})^{1/2} + 30\,(\chi_A - \chi_B)^2 \tag{9}$$

$$DC = 100 \exp\left[-(\chi_A - \chi_B)^2/4\right] \tag{10}$$

where, E_{A-A} and E_{B-B} are the energy of homeopolar bonds between atoms A, B and χ_A,χ_B are electronegativity of atoms. Table 6 shows that the degree of covalency is quite high (degree of covalency - DC) of all chemical bonds included in the studied ChG materials.

Table 5. Average bond energy ($\langle E \rangle, kcal/mol$), cohesive energy (CE, kcal/mol), Bond energy (kcal/mol)

Glass compositions	$\langle E \rangle$	**Cohesive energy (CE)**	**Bond energy**	**Bond energy**
$As_{40}Se_{60}$	49.44	41.2	As-S (45.18)	Se-Te (40.8)
$As_{40}Se_{30}Te_{30}$	44.34	36.95	As-Se (41.2)	Se-Se (44)
$As_{40}Se_{30}S_{30}$	51.828	43.15	As-Te (32.7)	Te-Te (33)
$As_{33.3}Se_{33.3}S_{33.4}$	51.0946	39.95	Te-S (47.25)	S-S (50.9)
$As_{33.3}Se_{33.3}Te_{33.4}$	43.3618	34.19	Se-S (47.47)	As-As (32.1)

Table 6. Degree of covalency (DC, %), Electronegativity (χ) in studied glasses

Glass compositions	**Degree of covalency**		**Electronegativity (χ)**	
$As_{40}Se_{60}$	As-Se	96,635		
$As_{40}Se_{30}Te_{30}$	As-Te	99,84	As	2.18
$As_{40}Se_{30}S_{30}$	As-S	96,07	Se	2.55
$As_{33.3}Se_{33.3}S_{33.4}$	Se-Te	95,06	Te	2.1
$As_{33.3}Se_{33.3}Te_{33.4}$	Se-S	99,977	S	2.58

Therefore, the results obtained can be interpreted by the theory developed for materials have covalent bonds. Applying the method proposed in [6], where, based on simple structural assumptions, taking into account the stoichiometry and using known values of the energy of interatomic bonds, the average values of bond energy of the As_xSe_{1-x} system are calculated, the average values of the bond energy of all the studied compounds are estimated, which results are presented in Table 5. The cohesive energy (CE) was calculated by using the basic principles the model of chemical bond approache (CBA) model [39], which the cohesive energy (CE) is the stabilization energy of an infinitely large cluster of material per atom and also reflects the average bond strength. According to CBA, the probability of the formation of heteropolar bonds exceeds the homeopolar bonds. Firstly, the most strong bonds are formed (due to high energies) and the sequence of the formation of these bonds corresponds to the sequence of decreasing energy until is satisfied the available atomic valence. Each constituent atom is coordinated by N- 8 atoms, where N - number of outer shell electrons, which neglects the presence of dangling bonds and other defects in the valence first approximation. The van-der-Waals interaction is also neglected, which can play a significant role in the process of stabilization of the material through the formation of weaker bonds than ordinary covalent bonds. Based on the CBA, the bonding energies are assumed to be additive. Thus, the CE was calculated by summing the energies of all the connection relations, the expected in the material and the results shown in Table 5.

4. Discussion

Research shows that, changes occurring in the width of the band gap can be interpreted in the framework of the model proposed by the author of [40] for band gap materials of ChG materials. The chemical bonds of chalcogenic atoms (S, Se, Te) with As atoms or between are formed via bonding (σ- molecular orbital), antibonding (σ* - orbital) orbitals and orbitals of a lonely pair of electrons (LP-orbital).In solid states, these orbits turn into bands. It is assumed that the LP – states form the top of the valence band and the σ* states form the bottom of the conduction band, so the energy distances betweem them corresponds to the width of band gap. As can be seen from table, the width of optical band gap for $As_{40}Se_{60}$ increases the by replacing part of the selenium atoms with sulfur but, decreaces replacing by the tellurium. The table also shows that the packing density of atoms almost remains constant, but the average the values of the bond energy undergoes a noticeable change, which must be accompanied by a change of the positions the edges allowed zones. Really, half of the chemical bonds Se-Se and As-Se existing in $As_{40}Se_{60}$ composition is replaced with bonds with high bond energies (in case of replacing part of selenium by sulfur), but is replaced with low bond energies (in case of replacing by tellurium) (Table 5). Consequently, the value of band gap strongly decrease in samples with tellurium (especially $As_{33.3}Se_{33.3}Te_{33.4}$) which, can be explained by the fact that both σ* orbitals and LP-orbitals belonging to Te – Te, Se-Te bonds (the relative fraction of such bonds will be high in chalcogen-rich compounds) fall into the gap of selenium mobility and leads to an increase in the tails of the edge zones [19], as a result decreases the optical band gap. The table also shows that there is a correlation between the width band gap and the average value of the bond energy, as well as the cohesive energy of the studied compositionsi.e. the value of these parameters increases when partially replacing of selenium with sulfur, while decreases partially replacing of selenium with tellurium.The parameter B in equations (2) depends on the material of the films and characterizes the slope of the absorption edge corresponding to the Tauc rule. The specified parameter is considered as a size of the degree disorder in non-crystalline materials [41-42,50]. The high values of the parameter $B^{1/2}$ in the ChG stoichiometric composition ($As_{40}Se_{60}$, $As_{40}Se_{30}S_{30}$, $As_{40}Se_{30}Te_{30}$, Table 1) indicate the perfection of their amorphous matrix. Otherwise, the low values of this parameter in ChG compositions chalcogen rich ($As_{33..3}Se_{33.3}S_{33.4}$, $As_{33.3}Se_{33.3}Te_{33.4}$ Table 1) indicate a high degree of disorder in the arrangement of atoms. Really, the spectrum of Raman scattering studies [22, 23] have shown that in these compositions the relative fraction of homopolar bonds between chalcogenide atoms is noticeably larger, as a result of which the density of local states increases near the allowed bands[19]. The dependence of the absorption coefficient on the energy photo the expressed by Urbach rule (3) near the absorption edge was observed in many chalcogenide glasses. There are different opinions [19,43-45,47,50] on the nature of the exponential dependence of the absorption coefficient on the photon energy. Authors of the article [45] the nature of the exponential dependence of the absorption coefficient are associate with random fluctuations of the internal field caused by structural disturbances inherent in amorphous materials.According to the author of [44,50], it is connected by electronic transitions between localized states located near the edges of the zone, whose density exponentially depends on energy.Mott and Davis [47] expressed against this opinion and considered the argument that the slope of the exponential behavior is constant for many crystalline and non-crystalline materials. The study carried out by us have shown that the values of Urbach energy (U) undergo a significant change with a change in the chemical composition of the studied ChG materials. Therefore, we believe that it is associated with a band width of localized states at the edges of the allowed bands of material and represents the degree of disorder in the chalcogenide glassy material. It is assumed that the absorption in this area is due to electronic transitions between the states (extended states) of one allowed zone and localized states the exponential tail belonging to another zone . As can be seen from Table 1 the highest values of Urbach energy are obtained for ChG composition containing tellurium. In this case, the most high values have been achieved for samples rich tellurium $As_{33,3}Se_{33,3}Te_{33,4}$ composition. As already noted,

the σ*- orbitals and LP - orbitals of the Te – Te and Se-Te bonds fall into the selenium mobility gap and lead to a decrease in the band gap and an increase in the exponential tail of localized states.

The temperature dependence of the Urbach absorption edge is related to the electron-phonon interaction (electron-phonon interaction (EPI)), which the firstly have been formed for ionic crystals [48]. The study of the photoinduced structural change (PSC) and the photodarkening effect revealed that a strong EPI exists in both crystalline and amorphous chalcogenides [19, 49-51].

The EPI parameters are obtained from the temperature dependence of the steepness parameter of the absorption edge (Fig. 3) by using the formula [50]:

$$\sigma = \sigma_0 \left[\frac{2kT}{\hbar\omega_p}\right]\tanh\left[\frac{2kT}{\hbar\omega_p}\right] \qquad (11)$$

where, $\hbar\omega_p$ -is the effective phonon energy in one oscillator model describing EPI, σ_0 -is a parameter independent of temperature and dependent on the glass material and characterizing the degree of steepness the Urbach absorption edge. The value of $\hbar\omega_p$ is determined from the Raman scattering spectrum (Fig. 4), as the average vibrational energy of all chemical bonds entering the amorphous matrix, taking into account their percentage calculated using the basic principles of the CBA method. The numerical values of the parameter-σ_0 are calculated by formula (11). The values of both parameters are also presented in Tables 1,2.

As seen from the table, the values of parameter $\hbar\omega_p$ is smaller for samples containing tellurium, which is consistent with the results of work [50]. Table 2. shows that the numerical value of the parameter $\hbar\omega_p$ for ternary compositions ($As_{40}Se_{30}S_{30}$ and $As_{33,3}Se_{33,3}S_{33,4}$) is higher than for binary ($As_{40}Se_{60}$), which indicate strong EPI in complex ChG materialS [51].

The parameter -σ_0 characterizes the intensity of electron-phonon interactions in condensed metter. The author [53] expressed about the sharp transformation of an exciton from a free state to a self trapped state in halides of alkaline elements with σ_0= 1, which is confirmed by studies carried out in [54]. The values of σ_o<1 is evidence of the existence of EPI [55], which is performed for all studied ChG compositions presented in the Table1. The table also shows that for three-component samples, the value of σ_o is less than for $As_{40}Se_{60}$, which agrees with the opinion of a high degree EPI in multicomponent chalcogenide glasses [42].

In addition, the table shows that there is a correlation between the parameters characterizing the Urbach absorption edge. Really, the increase in the energy width of the Urbach edge is accompanied by an increase in the effective energy of phonons and a decrease in the parameter the slope of the Urbach edge(σ_0). Such changes of these parameters are associated by changes in the degree of electron-phonon interaction and the degree of structural disorder in the arrangement of atoms. The glass transition temperature (Tg) is the temperature above which an amorphous matrix can have different structural configurations and below which the matrix is frozen into a relatively equilibrium structure. Therefore, it is reasonable to assume that the Tg should be associated with the parameters characterizing the amorphous matrix and determining the cohesive forces between the elements responsible for the stability of the amorphous structure. Among these parameters may include the average coordination number, the average bond energy, cohesive energy, etc. High values of the average bond energy and cohesive energy, which are a function of the coordination number, the type and energy of the bond and the degree of crosslinking prevent the decays of structural elements and the creation of mobile objects. The parallel observation changes of Tg and the values of the indicated quantities depending on the chemical composition, makes it possible to reveal the connection between them and express the possibility of directionally changing the properties of ChS materials. For the firt time, the authors of [16] are established empirically relationship between glass transition temperature and the average bondenergy for binary and ternary chalcogenide glasses.

$$T_g = 311[\langle E\rangle - 0{,}9] \qquad (12)$$

where $\langle E\rangle$ is value of the average bond energy.

Using data <E>, shown in Table 5 are calculated values Tg and the results of these calculations are presented in Table 3, which also shows the experimentally obtained values of Tg. As seen from the table, there is a good correlation between the experimental and calculated values. The value of Tg increases as a result replacing a part of selenium atoms with sulfur ($As_{40}Se_{30}S_{30}$ and $As_{33.3}Se_{33.3}S_{33.4}$) and decreases replacing with tellurium ($As_{40}Se_{30}Te_{30}$ and $As_{33.3}Se_{33.3}Te_{33.4}$). Such a change in the values of Tg, the average value of the bond energy, cohesive energy is due to changes occurring in the chemical bonds that form the amorphous matrix. In the first case, some of the As-Se and Se-Se chemical bonds in $As_{40}Se_{60}$ are replaced with bonds with high energy, i.e. As-S, S-S and Se-S bonds and in the second case with bonds lower energy, i.e. As-Te, Te-Te and Se-Te connections (Table 5). Moreover, in the second case, the greatest changes are observed in the values of these quantities, which are due to the lowest values of bond energy between atoms involving tellurium atoms. The table shows that the value of Tg in samples of non-stoichiometric $As_{33,3}Se_{33,3}S_{33,3}$ and $As_{33,3}Se_{33,3}Te_{33,4}$ compositions are less than in $As_{40}Se_{30}S_{30}$ and $As_{40}Se_{30}Te_{30}$. This is due to the low value of the average coordination number of non-stoichiometric compositions (the value of Z is equal to 2.33). According to the topological theory [56–57], the glass transition temperature of chalcogenide glasses is directly related to the rigidity of the amorphous matrix, i.e. with the degree of crosslinking of polymer chains. At critical values, the average coordination number Z = 2.4 matrix from the floppy state goes into a rigit state. Therefore, the value of Tg for the samples stoichiometric compositions have a higher value than for non-stoichiometric compositions (Table 3). The expected

changes in the relative proportions of chemical bonds are confirmed by the study of Raman light scattering.

The above interpretation of the Raman spectrum light scattering showed that the $As_{40}Se_{60}$ matrix is formed from structural elements or molecular elements containing heteropolar bonds between As-Se atoms and in a small amount homopolar bonds between selenium and arsenic atoms. In the case of replacing part of selenium atoms with sulfur ($As_{40}Se_{30}S_{30}$ and $As_{33.3}Se_{33.3}S_{33.4}$ compositions), a new band appears in the spectrum and the characteristic maxima belong to structural elements, in which some of these bonds are replaced by high energies As-S, Se-S and S-S bonds (see Table 3). These changes in the amorphous matrix cause an increase the values of the average bond energy, cohesive energy, optical band gap and glass transition temperature (Tables 5, 2 and 3).

In the case of replacing a part of selenium atoms with tellurium ($As_{40}Se_{30}Te_{30}$ and $As_{33,3}Se_{33,3}Te_{33,4}$glasscompositions) are attenuated the bands connected by vibrations of bonds belonging to structural elements with participation of atoms selenium and instead appear new bands relating to structural elements containing As-Te, Se-Te and Te-Te, which they have low bond energies (Table.5). Therefore, it is observed a significant decrease of the above listed parameters.

It is well known that the glass transition temperature(Tg) is mainly depends on the chemical bonds of the amorphous structure and increases with increasing connectivity and hardness of the glassy matrix [58]. These features of the chalcogenide glassy matrix, along with the dependence on the energy characteristics of the matrix (CE, MBE, etc.), also directly depend on the parameters of the microstructure, in particular, on the number, types of the nearest neighbors of atoms and the distance between neighboring atoms. Their changes should be reflected in the numerical values of such parameters as the average value of the atomic volume (Va), packing density ($\varkappa$) and compactness (δ). The decrease of Va, δ and increase of $\varkappa$, causes an increase in the degree of connectivity and rigidity of the chalcogenide glassy matrix, which is accompanied by an increase of the glass transition temperature(Tg). As seen from the table in the stoichiometric $As_{40}Se_{60}$ compositions replacing half of the selenium atoms with sulfur ($As_{40}Se_{30}S_{30}$ composition) occurs imperceptible decrease in Va, δ and the growth of $\varkappa$ and the replacement of selenium atoms with tellurium ($As_{40}Se_{30}Te_{30}$ composition) causes a noticeable increase in Va and but a slight decrease in δ. These results are consistent with the results of neutron diffraction [22,59], where have shown that for the $As_{40}Se_{60}$, $As_{40}Se_{30}S_{30}$ and $As_{40}Se_{30}Te_{30}$ series the radius of the first and second coordination sphere and the diameters of the nano voids decrease for the second composition, but decrease for the third composition. The strongly changes in the parameters of the microstructure were observed in samples of nonstoichiometric compositions ($As_{33.3}Se_{33.3}S_{33.4}$ and $As_{33.3}Se_{33.3}Te_{33.4}$), where Va increases and $\varkappa$, δ decrease.

5. Conclusions

The amorphous films of $As_{40}Se_{60}$, $As_{40}Se_{30}Te_{30}$, $As_{40}Se_{30}S_{30}$, $As_{33,3}Se_{33,3}S_{33,4}$, $As_{33,3}Se_{33,3}Te_{33,4}$ glass compositions is obtained by thermally evaporation method in vacuum (residual pressure is ~$1.33x10^{-4}$ Pa) and have been studied by X-ray diffraction, optical and Raman spectroscopy methods. The changes of glass transition temperature depending on the composition have been studied by method differential scanning calorimetry (DSC). The optical studies shows that is highest values of Urbach energy for glass composition containing tellurium and the most high values have been achieved for samples rich tellurium $As_{33,3}Se_{33,3}Te_{33,4}$ composition. As a result, mentioned composition indicate a high degree of disorder in the arrangement of atoms, where the σ*- orbitals and LP - orbitals of the Te – Te and Se-Te bonds fall into the selenium mobility gap and lead to a decrease in the band gap and an increase in the exponential tail of localized states. It has been shown that the value of optical band gap(Eg) for $As_{40}Se_{60}$ increases from 1.82 to 2.1 by replacing part of the selenium atoms with sulfur but, decreaces from 1.82 to 1.3 by replacing the tellurium. The Raman spectrum of $As_{33.3}Se_{33.3}Te_{33.4}$ composition contains all the features found in the spectrum of $As_{40}Se_{30}Te_{30}$ differing from that peaks at 108 and 136 cm^{-1} and a band at 259 cm^{-1} are amplified. The analysis of results show that, this fact is due to the excess concentration of chalcogen atoms. The value of Tg increases as a result replacing a part of selenium atoms with sulfur ($As_{40}Se_{30}S_{30}$ and $As_{33.3}Se_{33.3}S_{33.4}$) and decreases replacing with tellurium ($As_{40}Se_{30}Te_{30}$ and $As_{33.3}Se_{33.3}Te_{33.4}$). Such a change in the values of Tg, the average value of the bond energy, cohesive energy is due to changes occurring in the chemical bonds that form the amorphous matrix. In the first case, some of the As-Se and Se-Se chemical bonds in $As_{40}Se_{60}$ are replaced with bonds with high energy, i.e. As-S, S-S and Se-S bonds and in the second case with bonds lower energy, i.e. As-Te, Te-Te and Se-Te connections (table 3). Moreover, in the second case, the greatest changes are observed in the values of these quantities, which are due to the lowest values of bond energy between tellurium atoms.

References

[1] A. Zakery, S. R. Elliott, Optical Nonlinearities in Chalcogenide Glasses and their Applications **IX**, Springer, 29 (2007).
[2] J. L. Adam, X. Zhang, Chalcogenide Glasses, Preparation, Properties and Applications, Woodhead Publishing, 24 (2013).
[3] K. Tanaka, K. Shimakawa, Amorphous Chalcogenide Semiconductors and Related Materials, Publ. Springer-Verlag New York, 121 (2011).
[4] Y. Trifonova, A. Stoilova, V. Ivanova, V. Lilova, P. Petkov, J. Chem. Technol. Metall. **55**(4), 810 (2020).
[5] A. M. Adam, E. Lilov, V. Lilova, P. Petkov, Mater.

Sci. Semicond. Process **57**, 210 (2017).
[6] G. Yang, B. Bureau, T. Rouxel et al., Phys. Rev. B **82**, 195206 (2010).
[7] M. Bauchy, M. Micoulaut, J. Non-Cryst. Solids **377**, 34 (2013).
[8] S. I. Simdyankin, S. R. Elliott, Z. Hajnal et al., Phys. Rev. B **69**, 144202 (2004).
[9] P. Srivastava, H. S. Mund, Y. Sharma, Physica B **406**, 3083 (2011).
[10] F. Y. Lin, O. Gulbiten, Z. Y. Yang, L. Calvez, P. Lucas, Journal of Physics D-Applied Physics **44**, 045404 (2011).
[11] J. Kalužný, D. Ležal, E. Mariani, J. Pedlíková, V. Labaš, 12th International scientific conference CO-MAT-TECH 2004, MtF STU Trnava, Trnava, 553 (2004).
[12] S. A. Dembovskii, Phys. Chem. Classes **10**, 73 (1969).
[13] J. P. De Neufville, H. K. Rockstad, in: Amorphous and Liquid Semiconductors **1**, ed. J. Stuke and W. Breng (Taylor and Francis, London, 419 (1974).
[14] L. Tich, H. Tich, V. Smrcka, Mater. Lett. **15**, 202 (1992).
[15] A. N. Sreeram, D. R. Swiler, A. K. Varshneya, J. Non-Cryst. Solids **127**, 287 (1991).
[16] L. Tich, H. Ticha, Journal of Non-Crystalline Solids **189**, 141 (1995).
[17] K. Tanaka, Glass transition of covalent glasses, Solid State Commun. **54**, 867 (1985).
[18] K. Tanaka, J. Non-Cryst Solids **35-36**, 1023 (1980).
[19] K. D. Tsendin, Moscow Science, 317 (1996).
[20] F. Urbach, Phys Rev. **92**, 1324 (1953).
[21] K. Shimakawa, J. Non-Cryst. Sol. **43**, 229 (1981).
[22] R. I. Alekberov, S. I. Mekhtiyeva, A. I. Isayev, M. Fabian, J. Non - Cryst. Sol. **470**(15), 152 (2017).
[23] R. I. Alekberov, S.I. Mekhtiyeva, G. A. Isayev et al., Semiconductors **48**, 823 (2014).
[24] G. Lucovsky, R. M. Martin, J. Non-Cryst. Solids **8-10**, 185 (1972).
[25] G. Delaizir, M. Dussauze, V. Nazabal et al., Journal of Alloys and Compounds **509**, 831 (2011).
[26] V. Kovanda, M. Vlcek, H. Jain, J. Non-Cryst. Solids **326-327**, 88 (2003).
[27] T. Cardinal, K.A. Richardson, H. Shim et al., J. Non-Cryst. Solids **256–257**, 353 (1999).
[28] C. Lopez, K. A. Richardson, R. Valee, Conference on Lasers and Electro-Optics, CLEO'04/San Francisco, (2004) CThP5.
[29] F. Wenger, A. V. Melnichuk, A. V. Stronsky, Photostimulated Processes in Chalcogenide Glassy Semiconductors and Their Practical Application Academ.periodika E, Kiev, 2007.
[30] A. Mendoza-Galvan, E. Garcia-Garcia, Y. V. Vorobiev, J. Gonzalez-Hernandez, Microelectron. Engin.**51–52**, 677 (2000).
[31] M. H. Brodsky, R. J. Gambino, J. E. Smithjr., Y. Yacoby, Phys. Status Solidi B **52**, 609 (1972).
[32] T. Usuki, K. Saitoh, M. Endo, O. Uemura, J. Non-Cryst. Sol.**205–207**, 184 (1996).
[33] W. Li, S. Seal, C. Rivero, C. Lopez, K. Richardson, A. Pope, A. Schulte, S. Myneni, H. Jain, K. Antoine, A. C. Miller, J. Appl. Phys. **98**, 053503 (2005).
[34] O. V. Khiminets, V. S. Gerasimenko et al., Zh. Prikl. Khim. **51**(7), 1522 (1978).
[35] V. Pamukchieva, A. Szekeres, K. Todorova et al., J. Non-Cryst. Solids **355**, 2485 (2009).
[36] Y. N. Trifonova, V. C. Ivanova, A. A. Stoilova, V. D. Lilova, Bulg. Chem. Comm. **48**(4), 624 (2016).
[37] L. Pauling, The Nature of the Chemical Bond, third ed., Cornell University Press, Ithaca, USA, 1960.
[38] Tauc, R. Grigorovici, A. Vancu, Phys. Status Solidi **15**, 627 (1966).
[39] J. Bicerano, S. R. Ovshinsky, J. Non-Cryst. Solid. **74**, 75 (1985).
[40] M. Kastner, Phys. Rev. Letters **28**(6), 355 (1972).
[41] M. Behera, P. Naik, R. Panda, R. Naik, Optical Materials **66**, 616 (2017).
[42] G. H Jung, H. Kong, J.B. Yeo, H.Y. Lee, J. Korean Ceramic Society **54**(6) 484 (2017).
[43] N. F. Mott, E. A. Davis, Electron processes in non-crystalline solids, M. Mir, 664 (1982)
[44] S. I. Mekhtieva, D. ShAbdinov, Development of Selenium Physics, Elm, Baku, 13 (2000).
[45] J. D. Dow, D. Redfield, Phys. Rev. B**5**, 594 (1972).
[46] M. Zanini, J. Tauc, J. Non-Cryst. Solids **23**, 349 (1977).
[47] E. A. Davis, N. F. Mott, Philos. Mag. **22**, 0903 (1970).
[48] H. Y. Fan, Phys. Rev. **82**, 900 (1951).
[49] B. G. Ëurbulak, S. Duman, A. Ates, Czech. J. of Physics **55**, 93 (2005).
[50] Y. Upsurge, Y. Mizushima, J. Appl. Phys. **5**, 1772 (1980).
[51] I. P. Studenyak, M. Kranjčec et al., Quantum Electronics Optoelectronics **19**, 371 (2016).
[52] H. Sumi, A. Sumi, J. Phys. Soc. Jpn. **56**, 2211(1987).
[53] Y. Toyozawa, Technical Report of the Institute for Solid State Physic, Ser. A No. 119 (1964)
[54] I. H. Kanzaki, S. Sakuragi, K. Sakamoto, Solid State Commun. **9**, 999 (1971).
[55] M. V. Kurik, Phys. Status Solidi A**8**, 9 (1971).
[56] C. Phillips, J. Non-Crystal. Solids **34**, 153 (1979).
[57] M. F. Thorpa, J. Non-Cryst. Solids **57**, 355 (1983).
[58] R. P. Wang, C. J. Zha, A. V. Rode, S. J. Madden, B. Luther-Davies, J. Mater. Sci.: Mater. Electron. **18**(1), 419 (2007).
[59] R. I. Alekberov, A. I. Isayev, S. I. Mekhtiyeva, M. Fábián, Physica B: Condensed Matter **550**, 367 (2018).

* Corresponding author: rahim-14@mail.ru